Study on Fuzzy Sliding Mode Active Disturbance Rejection Control Method for Horizontal Vibration of High-Speed Elevator Car System

Qinghua Ge, Lulu Zhang*, Hua Li, Qin He, Ruijun Zhang

School of Mechanical and Electrical Engineering, Shandong Jianzhu University, Jinan, Shandong, 250101,P.R. China
corresponding author :luzhanglu123@yeah.net

Abstract: To effectively control the horizontal vibration of high-speed elevator car system caused by the factors such as the irregularity of the guide rail and the nonlinearity of spring-damping in guide shoes, this paper proposes an active disturbance rejection (ADR) control method based on fuzzy sliding mode. Firstly, considering the nonlinear characteristics of the spring-damping in the guide shoes, the horizontal vibration dynamic model of the elevator car system is established. Then, the guide rail excitation and the linear and nonlinear disturbances of the car are summarized into the total disturbances of the car system, which can be estimated by the designed extended state observer. On this basis, a sliding mode active disturbance rejection (SADR) control is presented, which makes the anti-vibration and anti-disturbance control of the car system highly robust. For the chattering problem caused by sliding mode control, the fuzzy control method is designed to eliminate it, and the fuzzy sliding mode active disturbance rejection (FSADR) control for the horizontal vibration of the car system is further realized. Finally, MATLAB/Simulink is utilized for simulation tests. The simulation results show that, compared with ADR and SMADR, the root mean square value, maximum value and A95 peak value of horizontal vibration acceleration through FSADR are significantly reduced. Therefore, the FSADR control method designed in this paper can effectively suppress the horizontal vibration generated during the operation of high-speed elevators.

Keywords: High-speed elevator, horizontal vibration, active disturbance rejection control, sliding mode control, fuzzy control.

1. INTRODUCTION

The high-rise and super high-rise urban buildings require elevators to provide faster running speed. However, as the running speed of the elevator increases, the internal and external disturbances can increase dramatically, making it difficult to effectively control horizontal vibrations in the elevator car system (Zhou et al., 2022; Qiu et al., 2021). In addition, this will lead to poor riding comfort experience, and the service life of the elevator cannot be guaranteed (Ding et al., 2013; Qiu et al., 2020). How to effectively control the horizontal vibration of the car system during the high-speed operation has become one of the key technologies restricting the development of high-speed elevators.

To solve the problem of horizontal vibration control of the elevator car system, related experts and scholars have conducted relevant research (Wang et al., 2022; Zhang et al., 2019; Abdalla et al., 2018; Zhang et al., 2021). (Rajamani et al., 1999) proposed a PID controller for the multi-input and multi-output model of the elevator car system. (Xue et al., 2012) adopted the control method of combining generalized predictive control with traditional PID control, and verified through simulation that generalized predictive PID can effectively reduce the horizontal vibration of elevator. (Moazen et al., 2012) introduced two different PID control methods, compared their horizontal control effects on elevator maglev guidance system, and finally proposed a better PID control method to suppress horizontal vibration. (Colon et al., 2017) established a horizontal vibration model containing random uncertain guideway excitation, reduced the system vibration by applying horizontal active force, and compared the vibration effect with and without control through chaotic polynomial and K-L method. (Feng et al., 2009) built the horizontal vibration model of high-speed elevator, designed a robust controller using Lyapunov method and analyzed the effect with MATLAB/Simulink. (Nakano et al., 2011) constructed the optimal feedback method to control the horizontal vibration acceleration of the car system, which realized the suppression of the horizontal vibration of the elevator car system. (Yu et al., 2009) proposed an adaptive controller, which verified its effect on the horizontal vibration of the car through simulation. (He et al., 2022) proposed an adaptive sliding mode scheme to control the horizontal vibration of high-speed elevator car, and verified the effectiveness of the controller. In order to enhance the stability of elevator operation, (Hu et al., 2015) extended integer order PID to fractional order PID, and designed a fuzzy adaptive fractional order (PID mu) - D-lambda control. (Chen et al., 2020) constructed the state space equation of the elevator car system based on the linear fractional transformation method, and designed the optimal state feedback controller using the $H_2/H\infty$ method. (Cao et al., 2020) adopted linear matrix inequality (LMI) optimization technology, and the H_2/generalized H_2 hybrid control strategy is designed to improve the ride comfort of high-speed elevators. (Santo et al., 2018) proposed a control strategy based on Ricatti equation, and the simulation results showed that the proposed control strategy could effectively control the vibration response of the car system.

In the dynamic modeling of the elevator car system, the above research methods assumed that the model was an ideal and accurate model. The control systems did not consider the impact of its own design, installation uncertainty and external disturbances uncertainty on the model, so the methods mentioned above cannot effectively deal with the nonlinearity and complex disturbance problems in the car system. In practice, however, the disturbance factors such as guide shoe nonlinearity and guide rail irregularity are widely present in the model of high-speed elevator car system, resulting in significant nonlinearity, uncertainty and time-varying characteristics of the horizontal vibration response of the car system. Therefore, the influence of these factors should be considered in the vibration control of the elevator car system, especially for high-speed and ultra-high-speed elevators.

The active disturbance rejection control (ADR) method does not rely on the accurate model. It can not only use the extended state observer (ESO) to estimate the disturbance factors of the controlled system in real time, but also timely compensate them through the state error feedback (SEF). Then, the controlled object with disturbances and nonlinearity can be expressed by standard integral series type (Han, 2009; Gao, 2015; Jin et al., 2020). Therefore, aiming at the problem of horizontal vibration control of high-speed elevator car system, the active disturbance rejection control of elevator car system is designed to eliminate the influence of disturbances on the horizontal vibration. Due to the nonlinear and strong coupling characteristics of the disturbances in high-speed operation, the control accuracy and the adaptability to environmental changes of the state error feedback control law in ADR are difficult to meet the actual needs of the project, and the car after compensation still has obvious vibration. The sliding mode control is beneficial to improve the robustness of ADR, so a sliding mode ADR for elevator car system is designed. The fuzzy control is used to eliminate the steady-state error after sliding mode ADR control, so as to effectively reduce the chattering problem, and finally realize the fuzzy sliding mode ADR (FSADR) control of the high-speed elevator car system.

The remainder of this paper is constructed as follows. Section 2 establishes the dynamic model of the horizontal vibration of the high-speed elevator car system. Section 3 designs the active disturbance rejection (ADR) control, sliding mode active disturbance rejection (SADR) control and fuzzy sliding mode active disturbance rejection (FSADR) control of the car system. Simulation results for horizontal vibration control of the car system are given in Section 4. Then conclusions are drawn in Section 5.

2. DYNAMIC MODEL OF HORIZONTAL VIBRATION IN ELEVATOR CAR SYSTEM

The research object of this paper is the horizontal vibration of the elevator car system. In order to conform to the actual operation of the elevator as much as possible, the following assumptions are made (Wang et al., 2020). The car and car frame are rigid bodies, the rubber block is a linear spring-damping system, and the guide shoe is a nonlinear spring-damping system.

The horizontal vibration model of high-speed elevator car system is shown in Figure 1.

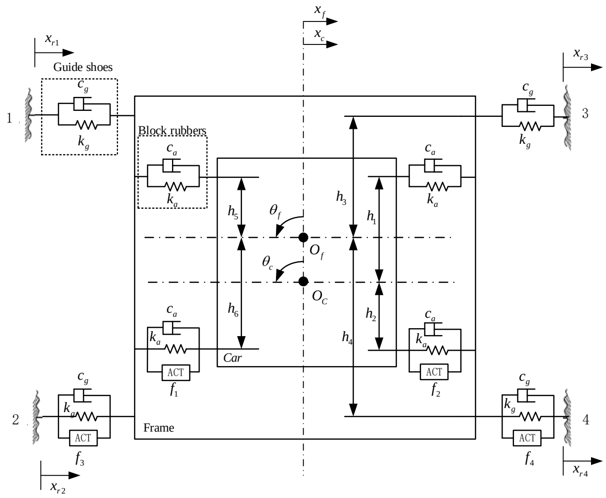

Fig. 1. Nonlinear horizontal vibration model of high-speed elevator car system.

The dynamic equation of horizontal vibration of high-speed elevator car system is established,

$$m_c\ddot{x}_c-\sum_{i=1}^{4}\left(k_{ai}\bullet z_i+c_{ai}\bullet \dot{z}_i\right)-f_1-f_2=0 \tag{1}$$

$$\begin{aligned}&I_c\ddot{\theta}_c+h_1\sum_{i=1,3}\left(k_{ai}\bullet z_i+c_{ai}\bullet \dot{z}_i\right)-h_2\sum_{i=2,4}\left(k_{ai}\bullet z_i+c_{ai}\bullet \dot{z}_i\right)\\&-h_2\bullet f_1+h_2\bullet f_2=0\end{aligned} \tag{2}$$

$$\begin{aligned}&m_f\ddot{x}_f+\sum_{i=1}^{4}\left(k_{ai}\bullet z_i+c_{ai}\bullet \dot{z}_i\right)-\sum_{i=1}^{4}\left(k_{gi}\cdot z_{gi}+c_{gi}\bullet \dot{z}_{gi}+d_i\right)\\&+f_1+f_2-f_3-f_4=0\end{aligned} \tag{3}$$

$$\begin{aligned}&I_f\ddot{\theta}_f-h_5\sum_{i=1,3}\left(k_{ai}\cdot z_i+c_{ai}\cdot \dot{z}_i\right)+h_6\sum_{i=2,4}\left(k_{ai}\cdot z_i+c_{ai}\cdot \dot{z}_i\right)\\&+h_3\sum_{i=1,3}(k_{gi}\cdot z_{gi}+c_{gi}\cdot \dot{z}_{gi}+d_i)-h_4\sum_{i=2,4}\left(k_{gi}\cdot z_{gi}+c_{gi}\cdot \dot{z}_{gi}+d_i\right)\\&+h_6\cdot f_1-h_6\cdot f_2-h_4\cdot f_3+h_4\cdot f_4=0\end{aligned} \tag{4}$$

where x_c is the horizontal displacement of the elevator car's center of mass, θ_c is the tilt angle of the car around its center of mass O_c, x_f is the horizontal displacement of the car frame's center of mass, and θ_f is the tilt angle of the car frame around its center of mass O_f . $c_{ai}(i=1,2,3,4)$ and $k_{ai}(i=1,2,3,4)$ represent the damping and stiffness coefficients of the rubber block , respectively. The guide rail irregularity excitation is $x_{ri}(i=1,2,3,4)$. f_1 and f_2 are the active control forces between the car and the car frame; f_3 and f_4 are the active control forces on the guide shoes, respectively. $k_{gi}(i=1,2,3,4)$ and $c_{gi}(i=1,2,3,4)$ are the linear stiffness and linear damping coefficients of the guide shoes, respectively. $d_i (i=1,2,3,4)$ describes the nonlinear characteristics of the guide shoe spring and damping:

$$d_i = k_{gli} \cdot z_{gi}^3 + c_{mi} \cdot \left| \dot{z}_{gi} \right| + c_{ni} \sqrt{\left| \dot{z}_{gi} \right|} \operatorname{sgn}\left(\dot{z}_{gi} \right), i = 1,2,3,4 \tag{5}$$

where $k_{gli} (i=1,2,3,4)$ are the nonlinear spring coefficients, c_{mi} and c_{ni} are the damping correction coefficients and damping nonlinear correction coefficients, respectively.

Actually, the change range of car and car frame around the center of mass tilt angle θ_c and θ_f is very small, so the displacement of car frame can be expressed as:

$$z_{g1} = x_{r1} + h_3 \sin\theta_f - x_f \approx x_{r1} + h_3\theta_f - x_f \tag{6}$$

$$z_{g2} = x_{r2} - h_4 \sin\theta_f - x_f \approx x_{r2} - h_4\theta_f - x_f \tag{7}$$

$$z_{g3} = x_{r3} + h_3 \sin\theta_f - x_f \approx x_{r3} + h_3\theta_f - x_f \tag{8}$$

$$z_{g4} = x_{r4} - h_4 \sin\theta_f - x_f \approx x_{r4} - h_4\theta_f - x_f \tag{9}$$

Similarly, the deformations of the rubber blocks $z_i (i=1,2,3,4)$ meet the following relationship:

$$z_1 = x_f + h_1 \sin\theta_c - h_5 \sin\theta_f - x_c \approx x_f + h_1\theta_c - h_5\theta_f - x_c \tag{10}$$

$$z_2 = x_f - h_2 \sin\theta_c + h_6 \sin\theta_f - x_c \approx x_f - h_2\theta_c + h_6\theta_f - x_c \tag{11}$$

$$z_3 = x_f + h_1 \sin\theta_c - h_5 \sin\theta_f - x_c \approx x_f + h_1\theta_c - h_5\theta_f - x_c \tag{12}$$

$$z_4 = x_f - h_2 \sin\theta_c + h_6 \sin\theta_f - x_c \approx x_f - h_2\theta_c + h_6\theta_f - x_c \tag{13}$$

3. DESIGN OF THE FSADR CONTROLLER FOR THE ELEVATOR CAR SYSTEM

The performance index for horizontal vibration of high-speed elevator car systems is the car horizontal vibration acceleration (Liu et al., 2020; Zhang et al., 2018), so the control objectives of the controller established are $\ddot{x}_c$ and $\ddot{\theta}_c$.

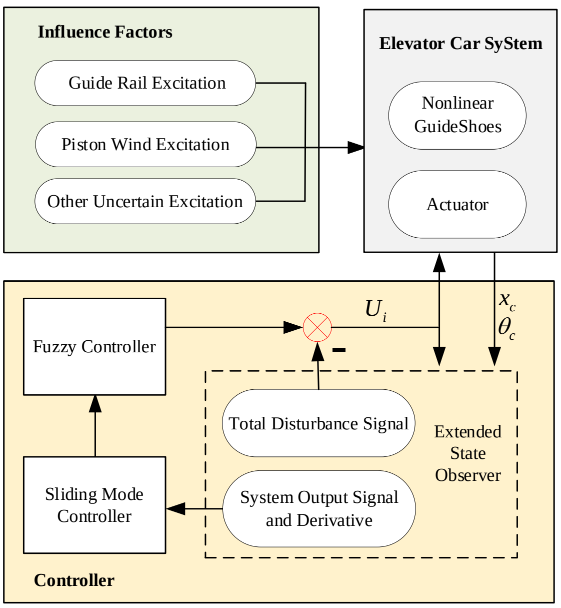

Fig. 2. FSADR block diagram of car horizontal vibration.

In this section, the fuzzy sliding mode active disturbance rejection (FSADR) control of the car system is designed. Firstly, the extended state observer (ESO) is constructed and the active disturbance rejection (ADR) control of the car system is designed. Then, the sliding mode active disturbance rejection (SADR) control of the car system is constructed to improve the robustness of the controller. Finally, the fuzzy sliding mode active disturbance rejection (FSADR) control is designed to compensate the factors that affect the horizontal vibration of the elevator car system as much as possible, that is, to minimize the values of x_c, θ_c and their accelerations. The FSADR control block diagram of the car system is shown in Figure 2.

3.1. *Design of the ADR controller applied to car system*

The extended state observer (ESO) in ADR can estimate the disturbances of the car system, which can be eliminated by state error feedback (SEF). ADR controller is designed as follows.

From equations (1) to (4), the following can be obtained

$$\begin{cases} \ddot{x}_c = g_1(*) + a_{11} f_1 + a_{12} f_2 + a_{13} f_3 + a_{14} f_4 \\ \ddot{\theta}_c = g_2(*) + a_{21} f_1 + a_{22} f_2 + a_{23} f_3 + a_{24} f_4 \\ \ddot{x}_f = g_3(*) + a_{31} f_1 + a_{32} f_2 + a_{33} f_3 + a_{34} f_4 \\ \ddot{\theta}_f = g_4(*) + a_{41} f_1 + a_{42} f_2 + a_{43} f_3 + a_{44} f_4 \\ y_1 = x_c, y_2 = \theta_c, y_3 = x_f, y_4 = \theta_f \end{cases} \tag{14}$$

where $g_i(*) = g_i\left(z_1, \dot{z}_1, z_{g1}, \dot{z}_{g1}, d_1, \cdots, z_4, \dot{z}_4, z_{g4}, \dot{z}_{g4}, d_4\right)$ is the total disturbances of the car system. The linear and nonlinear spring-damping of the guide shoe, linear rubber blocks, and guide rail excitation are included in the total disturbances. The equivalent control force $U_i (U_i = \sum_{i,j} a_{ij} f_i, i, j = 1,2,3,4)$ is introduced in the following form, that is, the operation sum of each active control force f_i is regarded as the equivalent control force.

$$\begin{bmatrix} U_1 \\ U_2 \\ U_3 \\ U_4 \end{bmatrix} = \begin{bmatrix} a_{11} f_1 + a_{12} f_2 + a_{13} f_3 + a_{14} f_4 \\ a_{21} f_1 + a_{22} f_2 + a_{23} f_3 + a_{24} f_4 \\ a_{31} f_1 + a_{32} f_2 + a_{33} f_3 + a_{34} f_4 \\ a_{41} f_1 + a_{42} f_2 + a_{43} f_3 + a_{44} f \end{bmatrix} = \mathbf{AF} \tag{15}$$

where $\mathbf{A} = \begin{bmatrix} \frac{1}{m_c} & \frac{1}{m_c} & 0 & 0 \\ \frac{h_2}{J_c} & -\frac{h_2}{J_c} & 0 & 0 \\ -\frac{1}{m_f} & -\frac{1}{m_f} & \frac{1}{m_f} & \frac{1}{m_f} \\ -\frac{h_6}{J_f} & \frac{h_6}{J_f} & \frac{h_4}{J_f} & -\frac{h_4}{J_f} \end{bmatrix}$, $\mathbf{F} = \begin{bmatrix} f_1 \\ f_2 \\ f_3 \\ f_4 \end{bmatrix}$.

The equivalent control force can be obtained by ADR, and then the active force of the car system can be further calculated.

Decouple the multi-input and multi-output elevator car system (14) into the following single-input and single-output integral series system

$$\begin{cases}\ddot{y}_1 = g_1(*) + U_1, y_1 = x_c \\ \ddot{y}_2 = g_2(*) + U_2, y_2 = \theta_c \\ \ddot{y}_3 = g_3(*) + U_3, y_3 = x_f \\ \ddot{y}_4 = g_4(*) + U_4, y_4 = \theta_f\end{cases} \tag{16}$$

For the four subsystems in equation (16), the disturbance acceleration $g_i(*)$ acting on the car system is expanded to a new state variable x_{i3}, and $\dot{x}_{i3}(t) = w(t)$ is recorded, then the expanded state system with disturbances is obtained

$$\begin{cases}\dot{x}_{i1} = x_{i2} \\ \dot{x}_{i2} = x_{i3} + U_i \\ \dot{x}_{i3}(t) = w(t) \\ \mathrm{y}_i = x_{i1}, i = 1,2,3,4\end{cases} \tag{17}$$

For the extended state, a linear extended state observer (LESO) is further designed as follows:

$$\begin{cases}\dot{z}_{i1} = z_{i2} + \beta_{i1}(y_i - z_{i1}) \\ \dot{z}_{i2} = z_{i3} + \beta_{i2}(y_i - z_{i1}) + U_i \\ \dot{z}_{i3} = \beta_{i3}(y_i - z_{i1}), \quad i = 1,2,3,4\end{cases} \tag{18}$$

where, z_{i1}, z_{i2} and z_{i3} are the outputs of ESO, estimating the system output signal y_i, the derivative $\dot{y}_i$ of the system output signal, and the total disturbance signal $g_i(*)$, respectively. The control signal U_i and system output y_i are the inputs of ESO. $\beta_{ij}, j = 1,2,3$ is the gain of the extended state observer, which can track the variables of the system and make the observation error smaller and smaller. That is, the estimated state is getting closer and closer to the real state, so that the estimated state and the real state completely overlap. To make the system stable, the observer is designed by pole assignment method. If all poles are selected at $\omega_{io}(\omega_{io} > 0)$, there is $\beta_{i1} = 3\omega_{io}, \beta_{i2} = 3\omega_{io}^2$ and $\beta_{i3} = \omega_{io}^3$, where the adjustable parameter ω_{io} is the observer bandwidth.

For the aforementioned elevator car system horizontal motion system equation (16), in order to obtain the output control force, the designed state error feedback control law is

$$U_{Ai} = k_{ip}(v_{i1} - z_{i1}) + k_{id}(v_{i2} - z_{i2}) - z_{i3}, i = 1,2,3,4 \tag{19}$$

where v_{i1} and v_{i2} are the reference input signals and their derivatives of the corresponding subsystems, respectively. The coefficients k_{ip} and k_{id} are defined as $k_{ip} = \omega_{ic}^2$ $k_{id} = 2\omega_{ic}$, where ω_{ic} is the controller bandwidth.

3.2 Design of the SADR controller

The car system ADR controller uses the ESO to estimate and compensate the total disturbances, so as to control the horizontal vibration of the car system. However, the SEF of ADR is essentially PD control. When facing the nonlinear and coupling complex car disturbances, it will produce a large overshoot, resulting in poor dynamic performance of the control. Therefore, the SEF in ADR needs to be modified. By sliding mode control, the system is forced to move into the designed sliding mode surface to enhance the disturbance rejection capability of ADR. The design of sliding mode controller consists of two steps: designing sliding mode surface and determining reaching law.

For the subsystem in equation (16), construct the slip surface function as

$$\mathbf{S} = \boldsymbol{\beta}\mathbf{E}_1 + \mathbf{E}_2 \tag{20}$$

where

$$\mathbf{S} = \begin{bmatrix} s_1 \\ s_2 \\ s_3 \\ s_4 \end{bmatrix}, \quad \mathbf{E}_1 = \begin{bmatrix} e_{11} \\ e_{21} \\ e_{31} \\ e_{41} \end{bmatrix}, \quad \mathbf{E}_2 = \begin{bmatrix} e_{12} \\ e_{22} \\ e_{32} \\ e_{42} \end{bmatrix}, \quad \boldsymbol{\beta} = \begin{bmatrix} c_1 & 0 & 0 & 0 \\ 0 & c_2 & 0 & 0 \\ 0 & 0 & c_3 & 0 \\ 0 & 0 & 0 & c_4 \end{bmatrix}$$

$-c_i(i = 1,\cdots,4)$ is the dynamic pole of sliding mode motion.

Select the constant reaching law, and the expression is $\dot{\mathbf{S}} = -\boldsymbol{\varepsilon}\mathrm{sgn}(\mathbf{S})$, where $\boldsymbol{\varepsilon} = \begin{bmatrix} \varepsilon_1 & 0 & 0 & 0 \\ 0 & \varepsilon_2 & 0 & 0 \\ 0 & 0 & \varepsilon_3 & 0 \\ 0 & 0 & 0 & \varepsilon_4 \end{bmatrix}$,

$\mathrm{sgn}(\mathbf{S}) = \begin{bmatrix} \mathrm{sgn}(s_1) \\ \mathrm{sgn}(s_2) \\ \mathrm{sgn}(s_3) \\ \mathrm{sgn}(s_4) \end{bmatrix}$, $\varepsilon_i\,(i = 1,2,3,4)$ are positive parameters,

and sgn represents a symbolic function.

Select Lyapunov function $V = (1/2)s^2$, $\dot{V} = s\dot{s} = s(-\varepsilon\,\mathrm{sgn}\,s) = -\varepsilon\,|\,s\,| \le 0$,then the sliding mode function $s \to 0$, thus tracking error $e_{i1} \to 0$. $e_{i1} = v_{i1} - y_i$, then $y_i \to v_{i1}$, that is, the actual output y_i of the car system can be tracked to the expected output v_{i1} under the action of the controller.

At the sliding mode surface, $\dot{\mathbf{S}} = \boldsymbol{\beta}\dot{\mathbf{E}}_1 + \dot{\mathbf{E}}_2 = 0$,then the equivalent control law is obtained as $u_{eqi} = c_i(v_{i2} - z_{i2}) + \ddot{v}_{i1} - z_{i3}, i = 1,2,3,4$.

The SADR control law is the sum of equivalent control and switching control, and the output of the controller is

$$U_{Si} = c_i(v_{i2} - z_{i2}) + \ddot{v}_{i1} - z_{i3} - \varepsilon_i sgns_i, i = 1,2,3,4 \tag{21}$$

3.3 Design of the FSADR controller

The sliding mode control is a discontinuous switching characteristic control in essence, which will cause chattering problem in the sliding mode surface of the control system. Then, a fuzzy sliding mode ADR controller for the car system is designed.

The fuzzy controller in this paper is Mamdani type. A single output and two inputs are used to form a two-dimensional fuzzy controller. The sliding mode switching surface function $s_i(t)(i=1,2,3,4)$ and its derivative $\dot{s}_i(t)$ are taken as the input variables of the corresponding fuzzy logic controller to produce the equivalent control force U_i. Define the fuzzy variables as

$$\begin{cases} e_{if}(t)=s_i(t)=e_{i2}+c_i e_{i1} \\ ec_{if}(t)=\dot{s}_i(t)=\dot{e}_{i2}+c_i\dot{e}_{i1} \end{cases} \tag{22}$$

The design of fuzzy controller is composed of four parts: fuzzification, knowledge base, fuzzy inference, and defuzzification. In order to increase precision and scope of application, the input variables take values in the interval [-6,6]. Using triangular membership functions, there are seven fuzzy subsets for both input and output variables, which are NB, NM, NS, ZO, PS, PM, and PB. The fuzzy inference rules are shown in Table 1. The fuzzy inference method is the Mamdani method, where "and" is taken as small, "or" is taken as large. The fuzzy implication adopts the smaller method, the fuzzy synthesis adopts the larger method, and the method of the center of gravity is used to solve the fuzzy. The quantization factors k_{ei} and k_{eci} are added before the D/F module and the scaling factor k_{ui} after the F/D module (D/F is a fuzzification module, and F/D is a defuzzification module). The two factors are collectively referred to as scale transformation factors.

Based on the above control rules, the surface observation of the logical relationship between the system inputs e, ec and the control outputs u is shown in Figure 3.

Table 1. Fuzzy inference rules table.

ec / *u* / *e*	NB	NM	NS	ZO	PS	PM	PB
PB	ZO	ZO	PS	PM	PM	PB	PB
PM	NS	ZO	ZO	PS	PM	PM	PB
PS	NS	NS	ZO	PS	PS	PM	PM
ZO	NM	NM	NS	ZO	PS	PM	PM
NS	NM	NM	NM	NS	ZO	PS	PS
NM	NB	NB	NM	NM	ZO	ZO	PS
NB	NB	NB	NB	NM	NS	ZO	ZO

Finally, a novel FSADR controller of the car system is obtained, and the specific structure is shown in Figure 4.

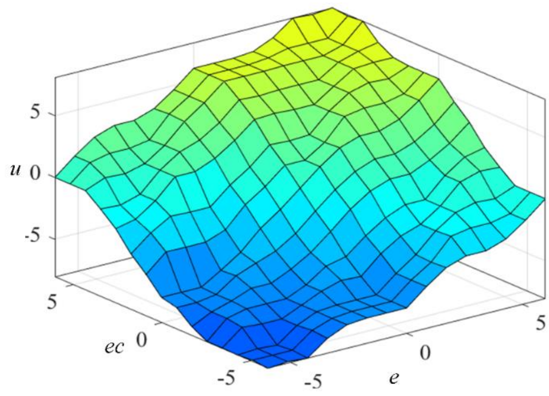

Fig. 3. Fuzzy regular surface diagram.

$$\begin{cases} \dot{z}_{i1}=z_{i2}+\beta_{i1}(y_i-z_{i1}) \\ \dot{z}_{i2}=z_{i3}+\beta_{i2}\left(y_i-z_{i1}\right)+U_i \\ \dot{z}_{i3}=\beta_{i3}\left(y_i-z_{i1}\right) \\ e_{if}=k_{ei}(c_i(v_{i1}-z_{i1})+v_{i2}-z_{i2}) \\ ec_{if}=k_{eci}(c_i(\dot{v}_{i1}-\dot{z}_{i1})+\dot{v}_{i2}-\dot{z}_{i2}) \\ u_i=\dfrac{\int x\mu_N(x)dx}{\int \mu_N(x)dx} \\ U_{Fi}=k_{ui}u_i-z_{i3} \\ (i=1,2,3,4) \end{cases} \tag{23}$$

where x is the fuzzy set domain, and $\mu_N(x)$ represents the membership.

4. SIMULATION ANALYSIS

To verify the effectiveness and feasibility of the fuzzy sliding mode active disturbance rejection (FSADR) control of the elevator car system designed in this paper, the simulation tests of the horizontal vibration of the 7m/s high-speed elevator car system are carried out using MATLAB/Simulink. The basic parameters of the controller are chosen as follows: the observer bandwidths are $\omega_{1o}=42$, $\omega_{2o}=50$, $\omega_{3o}=46$, $\omega_{4o}=43$,the controller bandwidths are , $\omega_{1c}=1.3$, $\omega_{2c}=2.3$, $\omega_{3c}=3.8$, $\omega_{4c}=1.5$, respectively. The detailed parameters of the high-speed elevator are shown in Table 2.

Guide rail excitation is the main factor causing horizontal vibration of high-speed elevator car (Crespo et al., 2018; He et al., 2021). Due to the inevitable machining errors and bending deformations during the processing of the guide rail, there must be some irregularities on the surface of the guide rail, resulting in random excitation of the car system. In addition, steps and surface notches of the rail joints can also generate impulse excitation. Therefore, this paper adopts two typical forms of random excitation and impulse excitation as the guide rail excitation.

Table 2. Parameters and physical significance in the elevator car system model.

Parameters	Unit	Value	Parameters	Unit	Value
Car moment of inertia I_c	$kg\times m^2$	1.8e3	Car frame moment of inertia I_f	$kg\times m^2$	2.8e3
Car mass m_c	kg	1.2e3	Car frame *mass* m_f	kg	7.5e2
Rubber block stiffness $k_{a1,2,3,4}$	N/m	2.0e5	Guide shoe linear stiffness $k_{g1,2,3,4}$	N/m	2.0e4
Rubber block damping $c_{a1,2,3,4}$	N×s/m	2.25e2	Guide shoe linear damping $c_{g1,2,3,4}$	N×s/m	1.0e2
Damping correction coefficients $c_{m1,2,3,4}$	N×s/m	20	Damping nonlinear correction coefficients $c_{n1,2,3,4}$	N×s/m	20
Nonlinear spring coefficients $k_{gl1,2,3,4}$	N/m	2.0e6	The vertical distance from the rubber block to the mass center of car h_1	m	1.17
The vertical distance from the rubber block to the mass center of car h_2	m	1.18	The vertical distance from the guide shoe to the mass center of car frame h_3	m	1.20
The vertical distance from the guide shoe to the mass center of car frame h_4	m	1.80	The vertical distance from rubber block to the mass center of car frame h_5	m	1.075
The vertical distance from rubber block to the mass center of car frame h_6	m	1.275	/	/	/

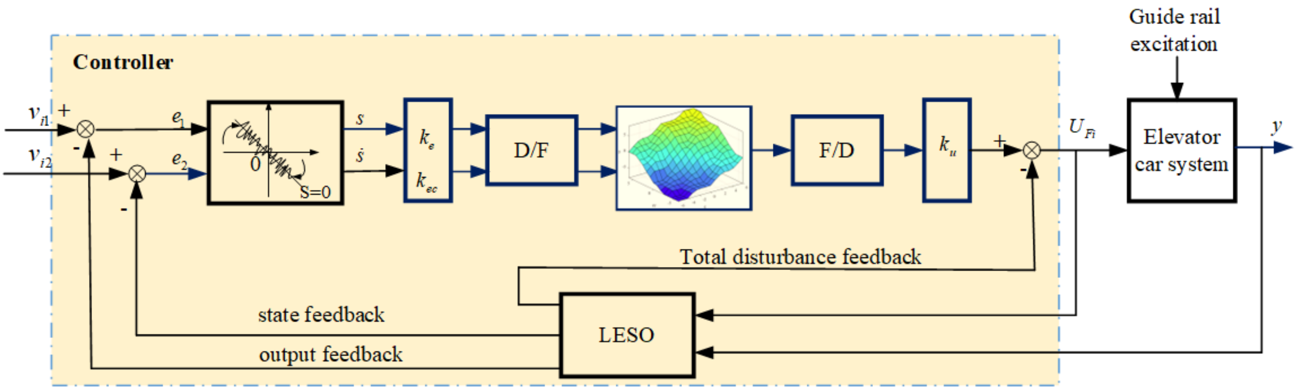

Fig. 4. Structure of FSADR controller.

4.1 Horizontal vibration control of elevator car system under random excitation of guide rail

The random excitation of the guide rail surface is Gaussian random process signal with mean value of 0 and standard deviation of 0.6 mm. Active disturbance rejection (ADR), sliding mode active disturbance rejection (SADR) and fuzzy sliding mode active disturbance rejection (FSADR) controllers are used to reduce the horizontal vibration of the car system respectively. The simulation test results are shown in Figures 5 and 6.

The change of horizontal displacement and tilt angle of elevator car system is shown in Figure 5. It is obvious to see that the FSADR controller can effectively reduce the horizontal displacement x_c and tilt angle θ_c, under the disturbances of nonlinear guide shoes and random excitation of guide rail. The vibration is significantly reduced, and the recovery time of the steady state is faster than the controllers ADR and SADR, that is, FSADR has good dynamic performance and strong robustness. The FSADR control effect of horizontal vibration is significantly better than that of ADR and SADR.

Figure 6 shows the time domain diagrams of the horizontal vibration acceleration $\ddot{x}_c$ and tilt angle acceleration $\ddot{\theta}_c$ of the car after control. As shown in Figure 6, the horizontal vibration acceleration of ADR and SADR has obvious fluctuations. The horizontal acceleration values and tilt angle acceleration values of FSADR elevator car are significantly smaller than those under ADR, indicating that the FSADR method proposed in the paper has advantages compared with ADR and SADR.

Figure 7 shows the frequency domain characteristics of horizontal vibration acceleration $\ddot{x}_c$ and tilt angle acceleration $\ddot{\theta}_c$. It can be seen that the peak value of low frequency amplitude of the car controlled by FSADR is significantly reduced, and the peak value of vibration is obviously controlled within the range of 1-3Hz.

Figure 8 compares the data distribution of horizontal displacement x_c and tilt angle θ_c under three controllers. The fluctuation of horizontal displacement and tilt angle controlled by ADR is maximum, and the data is unstable. The effect of SADR is better than that of ADR, while the control effect of FSADR is the best. The results show that the horizontal displacement and tilt angle of FSADR are stably controlled, and the horizontal vibration is effectively suppressed. Similarly, Figure 9 shows that the horizontal vibration acceleration $\ddot{x}_c$ and tilt angle acceleration $\ddot{\theta}_c$ are effectively controlled under FSADR control.

Tables 3 and 4 show the numerical responses of the three controllers for the car's horizontal vibration acceleration $\ddot{x}_c$ and tilt angle acceleration $\ddot{\theta}_c$ respectively. Compared with the uncontrolled values, the ADR reduces the MAX, RMS, peak-to-peak and A95 values of the car horizontal vibration acceleration by 28.5%, 37.1%, 29.2% and 37.2%, respectively, with a reduction in the range of 28.5% to 37.2%. The reduction range of SADR control is 51.5%~57.5%. The best control system is FSADR, which reduced the MAX and RMS values of horizontal vibration acceleration by approximately 60.4%~69.4%, a reduction of approximately 1.98 and 1.17 times that of the ADR and SADR controllers. These results further confirm the effectiveness and robustness of FSADR.

Similarly, Table 4 shows the control effect of tilt angle. The MAX, RMS, peak to peak value and A95 values of tilt angle obtained by ADR all decrease by 61.0%~65.9%. However, under the action of the SADR, these values are reduced by 73.6%~76.8%. The proposed FSADR control reduces these values by 75.0%~86.1%, which is approximately 1.26 times of the ADR control effect and 1.08 times of the FSADR control effect.

From the above analysis, it can be seen that after using FSADR control, the horizontal vibration values of the car under random excitation decrease most obviously, the dispersion of the data is small, and the peak-to-peak values descend significantly. The overall data shows that the FSADR is 1.61 times more effective than the ADR control and 1.12 times more effective than the SADR control, both indicating that FSADR control is the best of the three. The results show that the proposed FSADR active control has a great effect on suppressing horizontal vibrations generated by random guideway excitation and improving smoothness, resulting in satisfactory car system performance, stable system attitude and improved ride comfort.

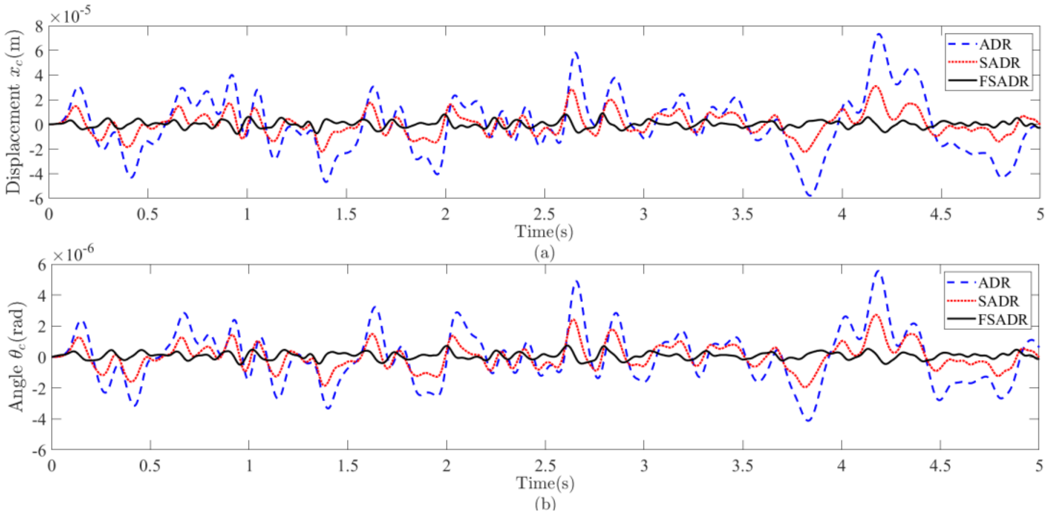

Fig. 5. Time domain response of horizontal displacement (a) and tilt angle (b) under random excitation.

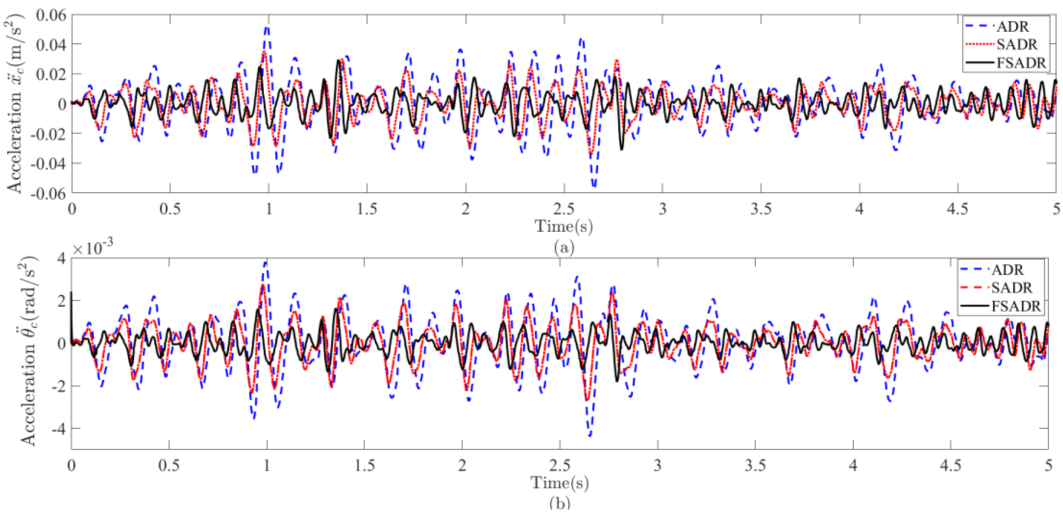

Fig. 6. Time domain response of horizontal vibration acceleration (a) and tilt angle acceleration (b) under random excitation.

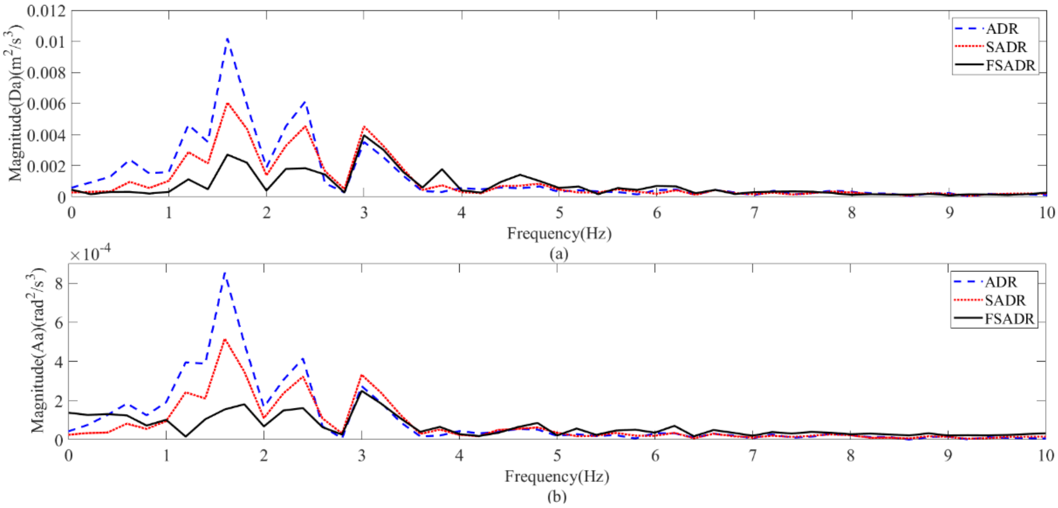

Fig. 7. Comparison of horizontal vibration acceleration (a) and tilt angle acceleration (b) in frequency domain under random excitation.

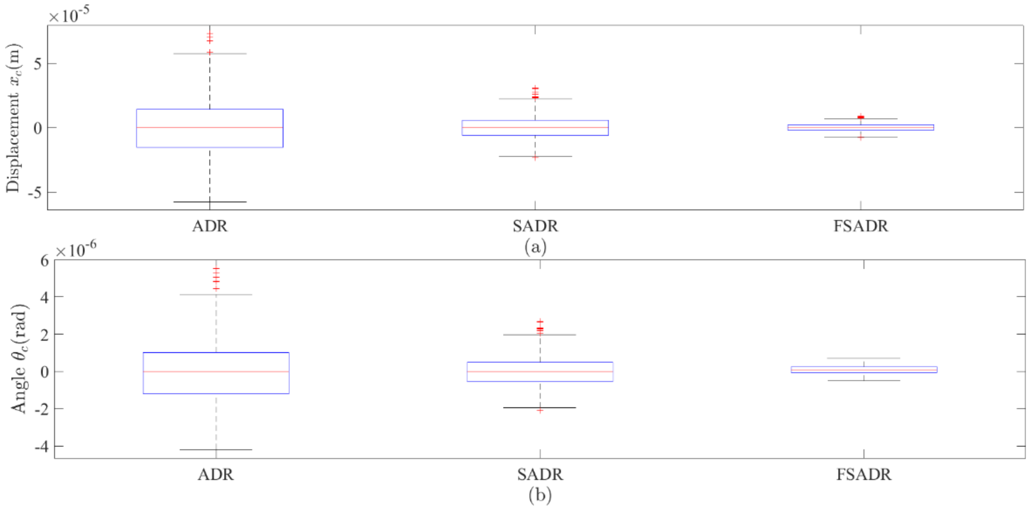

Fig. 8. Box plots of data distribution of horizontal displacement (a) and tilt angle (b) under random excitation.

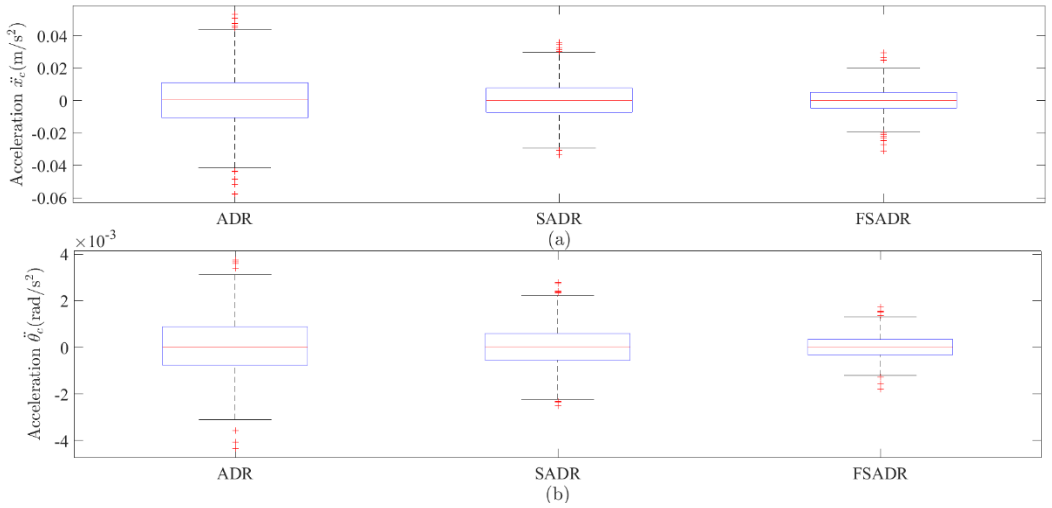

Fig. 9. Box plots of data distribution of horizontal vibration acceleration (a) and tilt angle acceleration (b) under random excitation.

Table 3. Comparison of horizontal vibration acceleration responses under random excitation.

Controller	Acceleration $\ddot{x}_c$(m/s^2)			
	MAX	RMS	Peak-to-peak	A95
Uncontrolled	0.0742	0.0258	0.1562	0.0416
ADR	0.0531 (↓28.5%)	0.0162 (↓37.1%)	0.1107 (↓29.2%)	0.0261 (↓37.2%)
SADR	0.0360 (↓51.5%)	0.0111 (↓56.9%)	0.0702 (↓55.1%)	0.0177 (↓57.5%)
FSADR	0.0294 (↓60.4%)	0.0079 (↓69.4%)	0.0605 (↓61.3%)	0.0133 (↓67.9%)

Table 4. Comparison of tilt angle acceleration responses under random excitation.

Controller	Acceleration $\ddot{\theta}_c$(rad/s^2)			
	MAX	RMS	Peak-to-peak	A95
Uncontrolled	0.0110	0.0036	0.0209	0.0059
ADR	0.0038 (↓65.9%)	0.0012 (↓64.9%)	0.0081 (↓61.0%)	0.0020 (↓65.6%)
SADR	0.0028 (↓74.8%)	0.0009 (↓75.6%)	0.0055 (↓73.6%)	0.0014 (↓76.8%)
FSADR	0.0024 (↓78.2%)	0.0005 (↓86.1%)	0.0052 (↓75.0%)	0.0008 (↓85.8%)

4.2 Horizontal vibration control of elevator car system under impulse excitation of guide rail

In this subsection, the impulse excitation with an amplitude of 5mm is designed. Simulation tests compare the suppression effects of ADR, SADR and FSADR on the horizontal vibration of the car system. The impulse signal is shown in Figure 10.

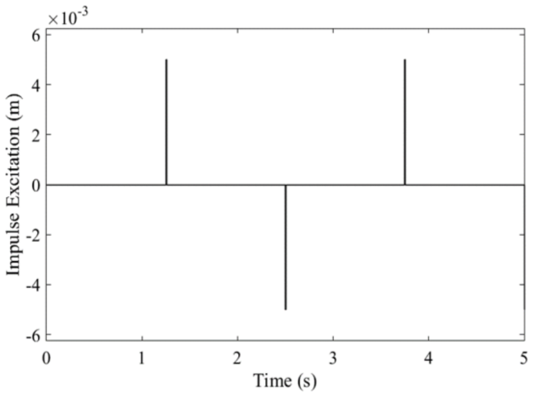

Fig. 10. Impulse excitation signal of the guide rail.

Under the impulse signal disturbances, Figure 11 compares the displacement x_c and tilt angle θ_c changes of the car horizontal vibration. It can be seen that the horizontal vibration of ADR and SADR is obvious. FSADR control can significantly reduce the peak value of the car horizontal displacement and tilt angle. Meanwhile, FSADR can reach the stable state faster and has stronger robustness.

As can be seen from Figure 12, compared to ADR and SADR, the car horizontal vibration acceleration $\ddot{x}_c$ and the tilt angle acceleration $\ddot{\theta}_c$ are both controlled to a certain extent by FSADR, with faster convergence times and smaller fluctuations. The performance of SADR is better than that of ADR. But for impulse excitation, FSADR has better suppression effect in the vibration process of elevator car system, which can make the system recover smoothly faster and is not vulnerable to disturbance.

Table 5 and Table 6 show the numerical comparison of horizontal vibration acceleration $\ddot{x}_c$ and tilt angle acceleration $\ddot{\theta}_c$ of high-speed elevator car under impulse excitation. In Table 5, compared with the uncontrolled controller, the horizontal acceleration RMS values of the ADR controller, the SADR controller and the proposed FSADR are reduced by 42.8%, 58.0% and 66.0%, respectively. The overall control effect of FSADR is 1.71 times that of ADR, and 1.16 times that of SADR. In Table 6, compared with the uncontrolled controller, the reduction range after ADR controller is 23.4%~36.1%, and the reduction range under the action of SADR controller is 42.0%~56.3%. Compared with the other two controllers, the tilt angle acceleration of FSADR decreases by 54.0%~69.5%, and the reduction range is about 2.29 and 1.27 times that of ADR and SADR controllers. Therefore, FSADR has a good control effect on the guide rail impulse excitation. Through the above simulation analysis, the proposed FSADR has more effective control performance than ADR and SADR. It can be seen that FSADR can not only effectively suppress the horizontal vibration of the high-speed elevator car system, but also reduce the peak vibration and shorten the time to reach the steady state for disturbances such as the excitation of guide rail and guide shoe nonlinearity. The effectiveness of the proposed FSARD control method is fully proved, which shows that the method is suitable for the horizontal vibration control of high-speed elevators.

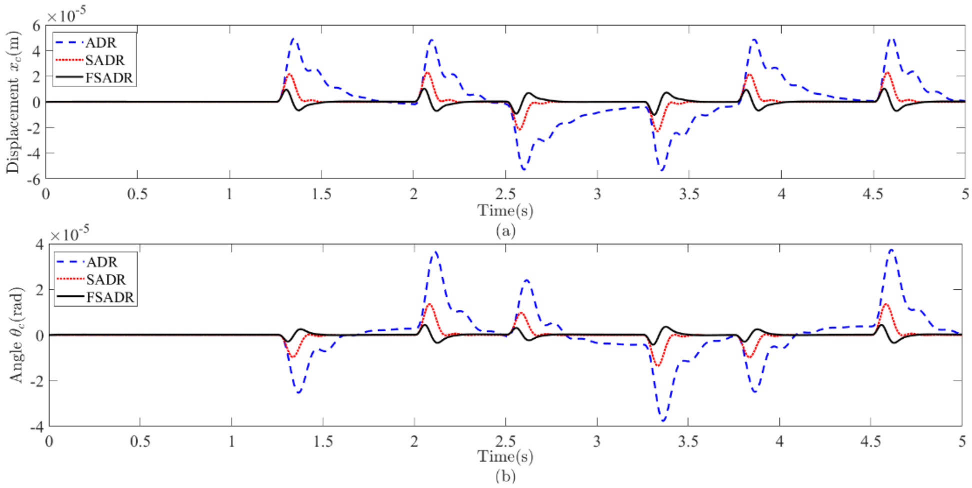

Fig. 11. Comparison of horizontal displacement (a) and tilt angle (b) under impulse excitation.

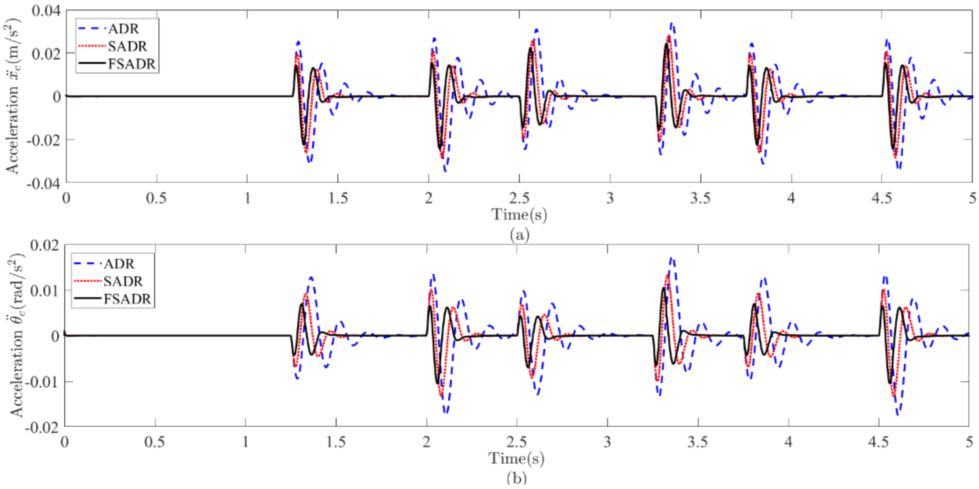

Fig. 12. Comparison of horizontal vibration acceleration (a) and tilt angle (b) acceleration under pulse excitation.

Table 5. Comparison of horizontal vibration acceleration responses under impulse excitation.

Controller	Acceleration $\ddot{x}_c$(m/s^2)			
	MAX	RMS	Peak-to-peak	A95
Uncontrolled	4.676E-02	1.773E-02	9.405E-02	3.373E-02
ADR	3.451E-02 (↓26.2%)	1.015E-02 (↓42.8%)	6.910E-02 (↓26.5%)	2.097E-02 (↓37.8%)
SADR	2.829E-02 (↓39.5%)	7.449E-03 (↓58.0%)	5.663E-02 (↓39.8%)	1.474E-02 (↓56.3%)
FSAD	2.442E-02 (↓47.8%)	6.032E-03 (↓66.0%)	4.878E-02 (↓48.1%)	1.254E-02 (↓62.8%)

Table 6. Comparison of tilt angle acceleration responses under impulse excitation.

Controller	Acceleration $\ddot{\theta}_c (\mathrm{rad/s^2})$			
	MAX	RMS	Peak-to-peak	A95
Uncontrolled	2.298E-02	7.560E-03	4.571E-02	1.269E-02
ADR	1.748E-02 (↓23.9%)	4.834E-03 (↓36.1%)	3.502E-02 (↓23.4%)	9.552E-03 (↓24.7%)
SADR	1.324E-02 (↓42.4%)	3.301E-03 (↓56.3%)	2.650E-02 (↓42.0%)	6.290E-03 (↓50.4%)
FSADR	1.049E-02 (↓54.3%)	2.307E-03 (↓69.5%)	2.101E-02 (↓54.0%)	4.341E-03 (↓65.8%)

5. CONCLUSIONS

This paper fully considers the influence of spring-damping nonlinearity and guide rail excitation in the guide shoes on the horizontal vibration of the high-speed elevator car system, and proposes an effective FSADR control method. The ADR control based on the extended state observer effectively estimates the disturbances such as the excitation of guide rail irregularity and the nonlinearity of the guide shoes. Combining the advantages of the sliding mode control, the SADR is designed to improve the robustness of the car horizontal vibration control and reduce the steady-state error. At the same time, the addition of fuzzy control solves the chattering problem of sliding mode control. Finally, through MATLAB/Simulink simulation, it is shown that FSADR makes the indexes such as the root mean square values and the maximum values of the horizontal vibration of the car decrease by more than 47%, and the numerical indexes of the tilt angle decrease by more than 54%. It is verified that the control method has favorable performance of vibration reduction and strong anti-disturbance ability under the effect of interference. In addition, the research results of this paper provide an important theoretical basis for the application of ADRC technology in other control problems.

ACKNOWLEDGEMENT

This work was supported by the Shandong Province Natural Science Foundation, China (grant number ZR2021ME245), and the Shandong Province Natural Science Foundation, China (grant number ZR2021ME210).

REFERENCES

Abdalla, M., Al-Jarrah, T. (2018). Optimal fuzzy controller: Rule base optimized generation. *Control Engineering and Applied Informatics*, Vol.20(2): 76-86.

Chen, C., Zhang, R., et al. (2020). Mixed H2/H∞ guaranteed cost control for high-speed elevator active guide shoe with parametric uncertainties. *Mechanics & Industry*, 21(5):502.

Cao, S., He, Q., Zhang, R., et al. (2020). Active control strategy of high-speed elevator horizontal vibration based on LMI optimization. *Control Engineering and Applied Informatics*, 22(1):72-83.

Crespo, R., Kaczmarczyk, S., Picton, P., and Su, H. (2018). Modelling and simulation of a stationary high-rise elevator system to predict the dynamic inter-actions between its components. I*nternational Journal of Mechanical Sciences*, Vol. 137, 24–45.

Ding, B., Zhang, Y., Peng, X., Li, Q., Tang, H. (2013). A hybrid approach for the analysis and prediction of elevator passenger flow in an office building. *Autom. Constr*, 35, 69–78.

Diego, C., Americo, C., et al. (2017). On dynamic analysis and control of an elevator system using polynomial chaos and Karhunen-Loève approaches. *Procedia Engineering*, 199:1629-1634.

Feng, Y., Zhang, J., Zhao, Y. (2009). Modeling and robust control of horizontal vibrations for high-speed elevator. *JVC/Journal of Vibration and Control*, Vol.15(9): 1375-1396.

Gao, Z. (2015). Active disturbance rejection control: From an enduring idea to an emerging technology. *2015 10th International Workshop on Robot Motion and Control*, *Poznan, Poland*, pp. 269-282.

He, Q., Jia, T., Zhang, R., and Liu, L. (2022). Adaptive sliding mode control with fuzzy adjustment of switching term based on the Takagi-Sugeno model for horizontal vibration of the high-speed elevator cabin system. *Proceedings of the Institution of Mechanical Engineers, Part C: Journal of Mechanical Engineering Science*, 236(9):4503-4519.

Hu, Q., and Hu, Y. (2016). Study on Fuzzy Adaptive Fractional Order (PID mu)-D-lambda Control for Maglev Guiding System. *International Conference on Applied Mechanics, Mechatronics and Intelligent Systems*, pp. 469-474.

Han, J. (2009). From PID to active disturbance rejection control. *IEEE Transactions on Industrial Electronics*, Vol.56(3): 900-906.

He, Q., Zhang, P., Cao, S., et al. (2021). Intelligent control of horizontal vibration of high-speed elevator based on gas-liquid active guide shoes. *Mechanics and Industry*, Vol.22:2.

Jin, H., Song, J., Lan, W., et al. (2020). On the characteristics of ADRC: a PID interpretation. *Science China Information Sciences*, 63, 209201.

Liu, M., Zhang, R., Zhang, Q., et al. (2021). Analysis of the gas-solid coupling horizontal vibration response and aerodynamic characteristics of a high-speed elevator. *Mechanics Based Design of Structures and Machines*, 1-22.

Moazen, M., Sharifian, M. B. B., and Afshari, H. (2012). PID Control of Maglev Guiding System for Linear Elevator.*2012 IEEE 5th India International Conference on Power Electronics*, pp. 1-6.

Nakano, K., Hayashi, R., et al. (2011). Active Vibration Control of an Elevator Car Using Two Rotary Actuators. *Journal of System Design and Dynamics*, 5. 155-163. 10.1299/jsdd.5.155.

Qiu, L., Zhou, H., Wang, Z., Zhang, S., Zhang, L., Lou, W. (2021). High-Speed Elevator Car Air Pressure Compensation Method Based on Coupling Analysis of Internal and External Flow Fields. *Applied Sciences*, Vol.11(1700): 1700.

Qiu, L., Wang, Z., Zhang, S., Zhang, L., and Chen, J. (2020). A Vibration-Related Design Parameter Optimization Method for High-Speed Elevator Horizontal Vibration Reduction. *Shock and Vibration*, pp.20.

Rajamani, R., Remmers, T., Roberts, R. (1999). Elevator active guidance system having a model-based multi-imput multi-output controller. *United States Patent*,5,866,861.

Santo, D., Balthazar, J., et al. (2018). On nonlinear horizontal dynamics and vibrations control for high-speed elevators. *Journal of Vibration and Control*, 24(5):825-838.

Wang, Z., Qiu, L., Zhang, S., Su, G., Zhu, L., and Zhang, X. (2022). High-speed elevator car system semi-active horizontal vibration reduction method based on the improved particle swarm algorithm. *Journal of Vibration and Control*,0(0).

Wang, H., Zhang, M., Zhang, R., et al. (2021). Research on predictive sliding mode control strategy for horizontal vibration of ultra-high-speed elevator car system based on adaptive fuzzy. *Measurement and Control* ,54(3-4):360-373.

Xue, J., Feng, Y., and Wu, H. (2012). Study on active control of horizontal vibration for high-speed elevators based on generalized predictive PID. *Mechanical Science and Technology for Aerospace Engineering*, 31(8), 1222-1226.

Yu, H., Zhang, and Dong, X. (2009). A novel adaptive control for elevator system with observer and parameter identification. *2009 IEEE International Conference on Automation and Logistics*, pp. 628-631.

Zhou, H., Zhang, S., Qiu, L., Wang, Z., and Li, H. (2022). The multi-component coupling horizontal vibration modeling technology of the high-speed elevator and analysis of its influencing factors. *Proceedings of the Institution of Mechanical Engineers, Part C: Journal of Mechanical Engineering Science*, 236(11):5850-5869.

Zhang, Q., Yang, Z., Wang, C., Yang, Y., and Zhang, R. (2019). Intelligent control of active shock absorber for high-speed elevator car. *Proceedings of the Institution of Mechanical Engineers, Part C: Journal of Mechanical Engineering Science*, 233(11):3804-3815.

Zhang, H., Zhang, R., He, Q., and Liu, L. (2021). Variable Universe Fuzzy Control of High-Speed Elevator Horizontal Vibration Based on Firefly Algorithm and Backpropagation Fuzzy Neural Network. *IEEE Access*, vol. 9, pp. 57020-57032.

Zhang, R., Wang, C., Zhang, Q. (2018). Response analysis of the composite random vibration of a high-speed elevator considering the nonlinearity of guide shoe. *Journal of the Brazilian Society of Mechanical Sciences and Engineerin*g, Vol.40(4): 190.